EUROPEAN FUSION DEVELOPMENT AGREEMENT

EFDA–JET–PR(04)38

H. Weisen, A. Zabolotsky, C. Angioni, I. Furno, X. Garbet, C. Giroud,
H. Leggate, P. Mantica, D. Mazon, J. Weiland, L. Zabeo, K.-D. Zastrow
and JET-EFDA contributors

Collisionality and Shear Dependences of Particle Pinches in JET and Extrapolation to ITER

Collisionality and Shear Dependences of Particle Pinches in JET and Extrapolation to ITER

H. Weisen[1], A. Zabolotsky[1], C. Angioni[2], I. Furno[3], X. Garbet[4], C. Giroud[5], H. Leggate[5], P. Mantica[6], D. Mazon[4], J. Weiland[6], L. Zabeo[4], K.-D. Zastrow[5] and JET-EFDA contributors*

[1]Centre de Recherches en Physique des Plasmas, Association EURATOM - Confédération Suisse, EPFL, 1015 Lausanne, Switzerland
[2]Max-Planck-Institut für Plasmaphysik, IPP-EURATOM Association, D-85748 Garching
[3]Los Alamos National Laboratory, Los Alamos, New Mexico 87545, USA
[4]Association EURATOM-CEA sur la Fusion, CEA-Cadarache, France
[5]EURATOM/UKAEA Fusion Association, Culham Science Centre, Abingdon, Oxon. OX14 3DB, UK
[6]Istituto di Fisica del Plasma, Associazione EURATOM-ENEA-CNR, Milano, Italy
[7]EURATOM-VR Association, Göteborg, Sweden
** See annex of J. Pamela et al, "Overview of Recent JET Results and Future Perspectives", Fusion Energy 2002 (Proc. 19th IAEA Fusion Energy Conference, Lyon (2002).*

Preprint of Paper to be submitted for publication in
Nuclear Fusion

ABSTRACT.
Results from an extensive database analysis of JET density profiles show that the density peaking factor $n_{e0}/\langle n_e \rangle$ in JET H-modes increases form near 1.2 at high collisionality to around 1.5 as the plasma collisionality decreases towards the values expected for ITER. This result confirms an earlier observation on AUG. The density peaking behaviour of L modes is remarkably different from that of H modes, scaling with overall plasma shear as ($n_{e0}/\langle n_e \rangle \sim 1.5 l_i$), independently of collisionality. H-mode density profiles show no shear dependence, except at the lowest collisionalities. Evidence for L_{Te}, L_{Ti}, ρ^* or β dependences has been obtained neither in L nor in H-modes. Carbon impurity density profiles from Charge Exchange Spectroscopy are always less peaked than electron density profiles and usually flat in H modes. The peaking of the electron density profiles, together with the flatness of the impurity density profiles, are favourable for fusion performance if they can be extrapolated to ignited conditions.

1. DENSITY PROFILES IN H MODES

Peaked electron and fuel density profiles in reactor plasmas provide the advantage of higher reactivity, higher bootstrap fraction and stronger electron-ion coupling in the core, than obtained with flat density profiles at the same average density, albeit at the risk of impurity accumulation in the core. Since the H-mode density limit appears to be governed by the pedestal density, peaked density profiles may also help dispelling recent concerns [1] about the possibility of attaining sufficiently high densities for ITER [2] to achieve its design performance. Therefore the discovery of a clear collisionality dependence of in AUG [3] H-modes called for an independent verification in JET. The theoretically important effective collisionality defined as $\nu_{eff} = \nu_{ei}/\omega_{De} \sim 3(m_i/m_e)^{1/2}\varepsilon^{3/2}\nu^*_{ei}/q$ (assuming $k_\theta\rho = 1/3$), where ν_{ei} is the electron collision frequency and the curvature drift frequency ω_{De} is a rough estimate of the ITG growth rate, and is therefore expected to govern both anomalous diffusion and convection [3].

The collisionality dependence of the density peaking factors for a large representative set of stationary ELMy JET H modes and 'hybrid scenario H-modes' (which have moderate to high q_{95} and low core magnetic shear) is shown in Fig.1. The density profiles were evaluated from the JET multichannel far infrared interferometer with the SVD-I inversion method [4], which uses basis function extracted from the LIDAR Thomson Scattering (TS) profiles, using the Singular Value Decomposition (SVD). This method greatly reduces errors in the LIDAR TS profiles, while granting consistency with interferometry. The collisionalities obtained on JET extend to below those expected for the ITER reference H-mode, indicated by a vertical line. The different symbols in Fig.1 refer to classes of internal inductance, which is a robust measure of overall magnetic shear. The same data are plotted versus l_i in Fig.2. There is no discernible dependence on l_i, except for $\nu_{eff} \leq 0.25$. This is in contrast to L-modes in DIII-D[5], TCV[6][7] and JET[8], where magnetic shear (or the peakedness of the current profile) was found to be the most important parameter, irrespective of collisionality.

The data presented here contain a great variety of conditions with $1.7\times10^{19} \leq \langle n_e \rangle \leq 11\times10^{19} m^{-3}$, $3\times10^{-3} \leq \rho^* 9\times10^{-3}$, $2.3 \leq q_{95} \leq 6.5$, $0.7 \leq \beta_N \leq 2.6$, $4 \leq R/L_{Te}(0.5) \leq 9$, $0.6 \leq T_e(0.5)/T_i(0.5) \leq 1.7$,

$0.04 \leq V_{loop} \leq 0.55$ and combinations of heating methods with $P_{nbi} \leq 17$MW, $P_{rf} \leq 10$MW, $P_{lhcd} \leq 3$MW, including a minority of cases with substantial RF heating (P_{rf}/P_{tot} in the range 0.4-0.9 and near central deposition r/a~0.3). We found no additional dependence of peaking on $<n_e>$, nor on V_{loop}, P_{rf}/P_{tot}, β_N, ρ^*, T_e/T_i, L_{Te}, or L_{Ti}. Figures 3&4 show the same data resolved into classes of ρ^*, and R/L_{Te}, evaluated at r/a=0.5, illustrating this lack of further dependences. In Fig.4, to offer an alternative representation, we characterise density peaking by $R/L_n = R\mathrm{dln}(n_e)/dr$ at mid-radius. A slide show presenting further parameter (in)dependencies may be downloaded from [9]. The results also show that the Ware pinch cannot be held responsible for density peaking at low ν_{eff}, where the lowest values of V_{loop} are obtained. Similarly the lack of a dependence on $<n_e>$and the fraction of RF heating P_{rf}/P_{tot},which govern the penetration of beam neutrals and the relative magnitude of the beam particle source, show that the beam source profile and magnitude do not determine the density profile. The particle source due to deep penetration of edge neutrals is less important than beam fuelling still, by 1-2 orders of magnitude at mid-radius, as estimated using the KN1D code[10].

Figures allowing a side-by-side comparison of JET and AUG results are available from refs [9]&[11]. The peaking is slightly higher (by ~0.1) at ν_{eff} ~0.2 in JET than in AUG when the evaluation of ν_{eff} is based on the average Z_{eff} derived from Visible Bremstrahlung (VB), as in Figs 1-4. JET results are however brought into full agreement with AUG when the hollow Z_{eff} profiles measured by CXS are used. Z_{eff} inferred from CXS at r/a=0.5 is typically lower by a factor 1.6 than Z_{eff} from VB, shifting the ν_{eff} axis by the same factor.

Unlike electron density profiles, carbon density profiles in H-modes are rather flat or slightly hollow, as seen for three examples with different collisionalities in Fig.5. As a result, carbon concentration, n_c/n_e, profiles are hollow inside r/a~0.7, especially at low collisionality, when density profiles are most peaked (Fig.6). These impurity density profiles may result from a balancing of the neoclassical inward and outward convective terms arising respectively from the main ion density and ion temperature gradients [15]. Recent calculations using the Weiland model also show that anomalous inward convection is lower for carbon than for deuterium. Whether this favourable behaviour is shared by high Z impurities, such as the ITER divertor material tungsten, remains to be investigated.

2. DENSITY PROFILES IN L-MODES

In source-free MHD-quiescent L-mode plasmas with off-axis Lower Hybrid Current Drive (LHCD) at power levels up to 3.6MW the peaking increases as $n_{e0}/\langle n_e \rangle \cong 1.6 l_i$, (Fig.7) and is independent of ν_{eff}. The figure also shows that the carbon density profile from CXS, although not flat in this case, is significantly less peaked than the electron density profile. These experiments, reported in [8], have been reanalysed using the SVD-I method, showing that the peaking factor was previously underestimated by 25%. The density profiles remain peaked at zero loop voltage and negligible core particle source, as determined by KN1D [10], confirming investigations in fully current driven discharges in Tore Supra [12] and TCV [7]. As in the above H-modes, no dependence on L_{Te} was found.

We have extended the study to a variety of NBI and ICRH L-modes with a similar results, $n_{e0}/\langle n_e \rangle \approx 1.4 l_i$ and no discernible collisionality dependence. A subset of the discharges in Fig.7 has been analysed with respect to microinstabilities with the gyrokinetic code GS2 [13]. The main result is that the sign of the mode frequency is very sensitive to input parameters. We interpret this as an indication that the discharges are in a mixed ITG/TEM regime, where little or no anomalous thermodiffusion, and hence no L_{Te} dependence, is expected [14].

3. DISCUSSION.

The above observations pose welcome constraints on the theoretical understanding and on ongoing modelling efforts. Some observations can however be related to existing theories. The ν_{eff} dependence in H-modes, which are largely in the ITG regime, is in agreement with fluid modelling [3]. Positive shear L-modes and H-modes at low ν_{eff} have profiles which are consistent with Turbulent EquiPartition [5], as expected from purely diffusive transport of trapped particles in poloidal flux space, i.e $\Delta N/\Delta\Psi$ ~constant (where Δ_N is the number of particles in the interval $\Delta\Psi$) over most of the cross section. A theoretical difficulty is the existence of peaked density profiles at high ν_{eff} in L-modes, while, for high values of ν_{eff}, H-mode profiles are much flatter. Another difficulty is to understand why there is no evidence for a shear dependence for H-modes at $\nu_{eff}>0.2$, despite the expectance that the curvature pinch is the dominant convective mechanism when ITG's dominate [14].

It seems reasonable to assume that the differences are somehow linked to the nature of the underlying turbulence (ITG or TEM). The fundamental difference between L and H-modes is the edge pedestal, which appears to lead to flatter core density profiles, which is stabilising TEMs and destabilising for ITGs. At $\nu_{eff}<0.2$, however, the significant density gradient in H-mode would reduce ITG growth rates and destabilise TEMs, which may explain why a shear dependence similar to that of L-modes is observed. (Recent observations in TCV and AUG also suggest that the domains where scaling with ν_{eff}, repectively shear, is observed do not coincide neatly with the H and L-mode regimes). The L-modes reported above appear to be in a mixed ITG/TEM regime, not however in a regime dominated by TEMs, as can be produced in devices equipped with high power electron heating such as TCV and AUG. In these devices density profiles have been observed to flatten in response to strong central electron heating [16][12][14]. The phenomenon has been attributed to the destabilisation of TEMs, producing an outward thermodiffusive flux proportional to the mode growth rate [14].

The agreement between JET and AUG, together with the lack of significant dependencies on dimensionless parameters other than ν_{eff} (and l_i at the lowest ν_{eff}), suggests that an extrapolation to ITER should be possible. Assuming otherwise similar conditions, we expect $n_{e0}/\langle n_e \rangle \approx 1.5\pm0.2$ for the collisionality of the ITER reference H-mode, corresponding to $R/L_n \approx 4\pm1$ at mid-radius. This is proposed to apply to the initial, non-active phase of operation when hydrogen or helium will be used as working gases. Extrapolation to ignited conditions is however uncertain, because the large

electron heating power deposited in the core by α-particles may strongly destabilise TEMs, leading to flatter density profiles. The amount of net electron heating and their effect on TEMs will however be reduced by electron-ion coupling, for which smaller devices with high local electron heating power densities are not necessarily representative. The non-observation, so far, of density flattening in JET should not be taken as an indication that the phenomenon disappears in large enough devices, since it may be also due to a lack of electron heating power available in JET. The issue calls for dedicated experiments at low ν_{eff}, where the central electron heating is tailored as to emulate the net electron heating profile in ITER.

REFERENCES

[1]. K. Borrass et al., Nuclear Fusion **44** (2004) 752
[2]. V. Mukhovatov et al, Plasma Phys. Contr. Fusion **45** (2003) A235
[3]. C. Angioni et al, Phys. Rev. Lett. **90** (2003) 205003
[4]. I. Furno et al, (2004), accepted for Plasma Phys. Contr. Fusion*
[5]. D.R.Baker et al, Nuclear Fusion **40** (2000) 1003
[6]. H. Weisen et al, Nuclear Fusion **42** (2002) 136
[7]. A. Zabolotsky, et al, Plasma Phys. Contr. Fusion **45** (2003) 735
[8]. H. Weisen et al, Plasma Phys. Contr. Fusion **46** (2004) 751
[9]. http://crppwww.epfl.ch/~weisen/PUBLICATIONS/nf_letter_04_extras.pdf
[10]. B. Labombard, MIT PSFC report PSFC-RR-01-03 (2001)
[11]. X. Garbet et al (2004), accepted for Plasma Phys. Contr. Fusion (invited EPS 2004)
[12]. G.T. Hoang, et al, Phys. Rev. Lett. **90** (2003) 155002
[13]. M. Kotschenreuther et al, Comput. Phys. Commun. **88** (1995) 128
[14]. C. Angioni et al, Nuclear Fusion **44** (2004) 827
[15]. S.P. Hirshman and D.J. Sigmar, Nuclear Fusion **21** (1981) 1079
[16]. J. Stober et al., Nuclear Fusion **41** (2001) 1535

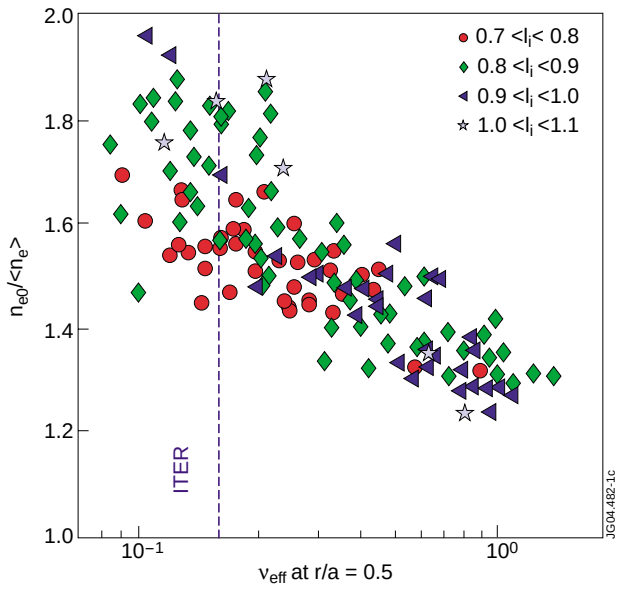

Figure 1: Density peaking factor in H-mode versus ν_{eff} at r/a=0.5. Symbols: classes of internal inductance l_i.

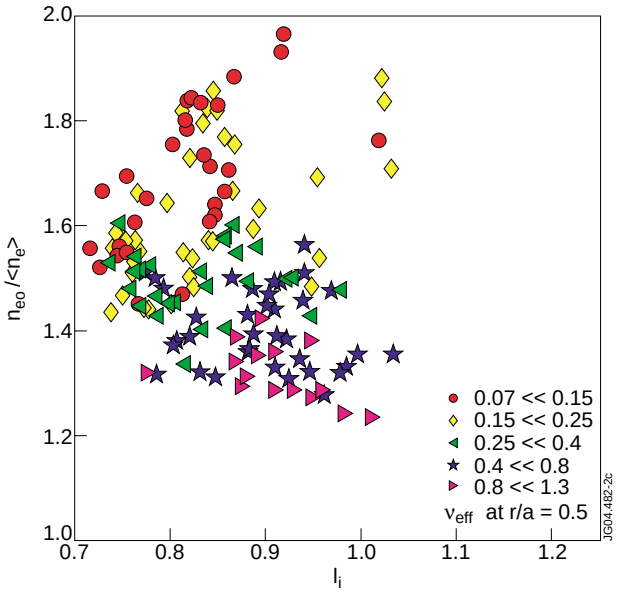

Figure 2: Peaking factor in H-mode versus l_i, resolved by classes of effective collisionality ν_{eff}.

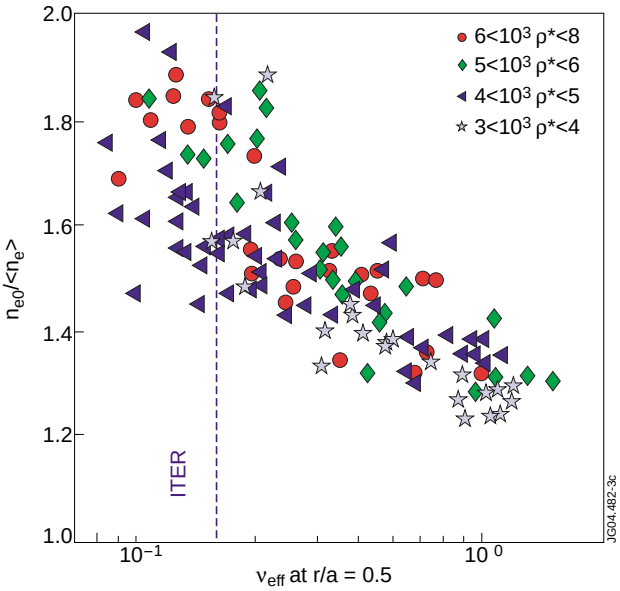

Figure 3: Peaking factor in H-mode versus ν_{eff}, resolved by classes of ρ evaluated at r/a=0.5.*

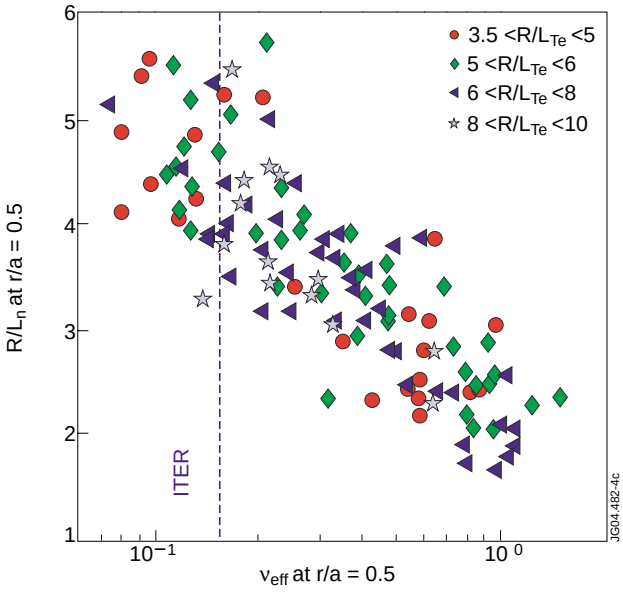

Figure 4: Normalised electron density gradient in H-mode at r/a=0.5 versus ν_{eff}, resolved by classes of electron temperature gradient.

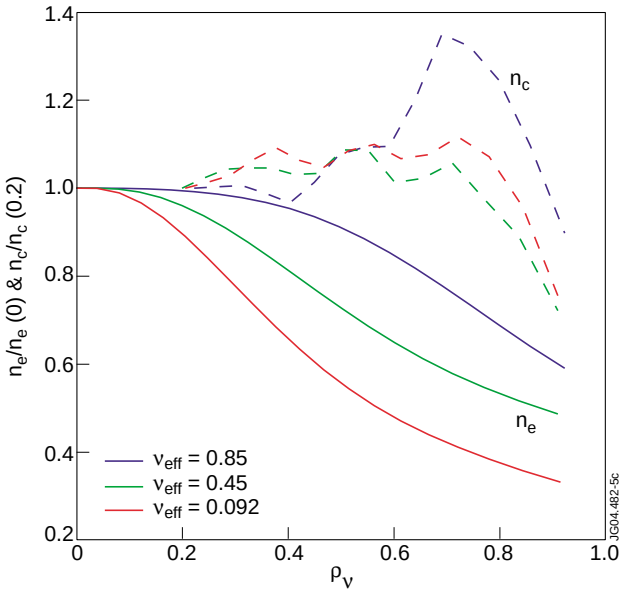

Figure 5: Normalised H-mode electron (-) and carbon impurity density (—) profiles for three different ν_{eff} and q_{95} ~3.

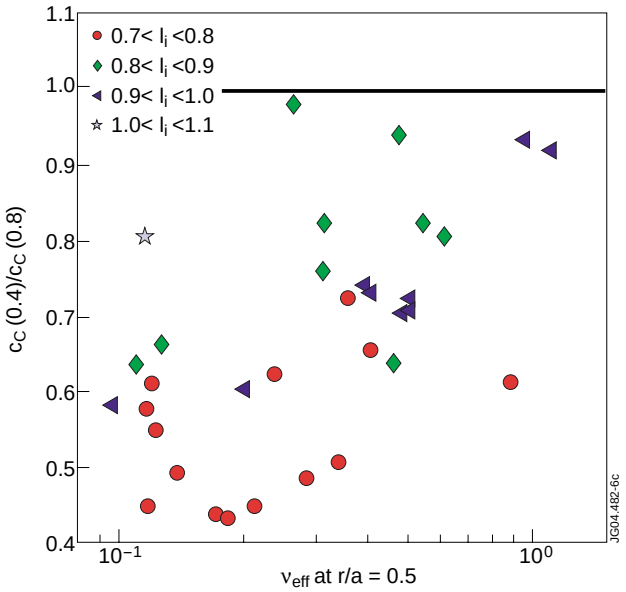

Figure 6: Ratio of carbon concentrations at r/a=0.4 and 0.8 as function of ν_{eff} in H-modes.

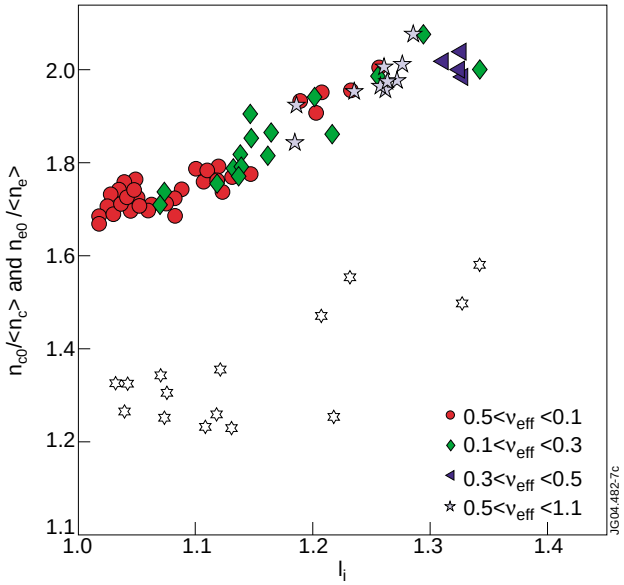

Figure 7: Density peaking in LHCD L-modes versus internal inductance, resolved by effective collisionality at r/a=0.5. Stars: Open Stars Carbon impurities.